Calculation of the Induced Currents and Forces for a Hybrid Magnetic Levitation System

D. Albertz, S. Dappen and G. Henneberger
Institut für Elektrische Maschinen, RWTH Aachen, Schinkelstraße 4, D-52056 Aachen, Germany

***Abstract*— This paper presents the calculation of the induced currents and forces for a 3D non-linear eddy current field problem with ferromagnetic moving conductors. The $\vec{A}$, V-$\vec{A}$ formulation is used in combination with four different gauging methods to stabilize the solution process. To consider non-rectangular shapes of geometries tetrahedral elements were employed. The computation procedure is applied to a hybrid magnetic levitation system of a contactless and frictionless conveyance system.**

I. Introduction

The calculation of braking and attractive forces for magnetic levitation systems is one of the basic demands for the design of levitation magnets. The calculated magnetic levitation system displayed in Fig. 1 consists of four hybrid magnets and a permanent excited linear synchronous machine with an iron-less stator [1]. To guarantee long operation periods and low energy consumption the currents of the hybrid excited magnets (NdFeB permanent magnets combined with an electrical excitation) are controlled to zero. The rail has a U-shape to use the reluctance force for the lateral guidance of the vehicle. To reduce material costs the rail is made of solid steel and does not suppress eddy currents. Since the stator is not designed over the whole length of the lane, eddy currents and the resulting braking effects caused by the motion of the vehicle have to be considered.

The attractive and propulsion forces are calculated by a mixed $\vec{A}$, V- $\vec{A}$ formulation [2]. This approach applied to moving conductor eddy current problems tends to stability problems in the solution process. An upwind scheme

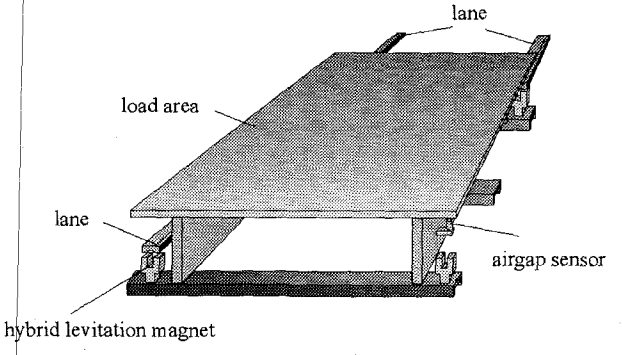

Fig. 1. Magnetic levitation system

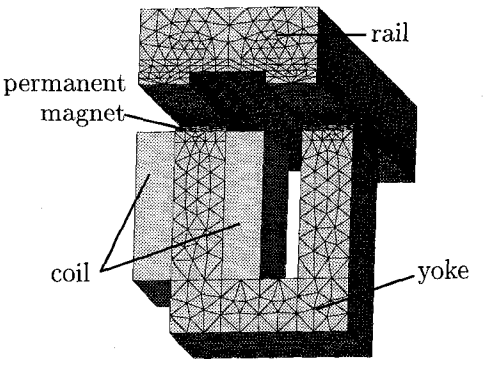

Fig. 2. Hybrid levitation magnet

and different gauging methods have been incorporated to achieve a stable, fast and precise solution. These methods will be compared with respect to solution time and accuracy. For this reason the induced currents and braking forces of one of the levitation magnets (Fig. 2) are calculated. In contrast to [3] 2D calculations can not be adapted by using different calculation parameters, so that a 3D calculation is absolutely required.

II. Formulation

A. Problem definition

The structure of the electromagnetic field problem of the hybrid levitation system is simplified shown in Fig. 3. To get a static field problem, the moving vehicle is chosen to be the local reference system of the electromagnetic model. So region Ω_1, representing the rail of the levitation system, is moving with a relative velocity to the fixed surrounding regions Ω_2 and Ω_3 representing the real moving parts of the geometry. Because the geometry of the

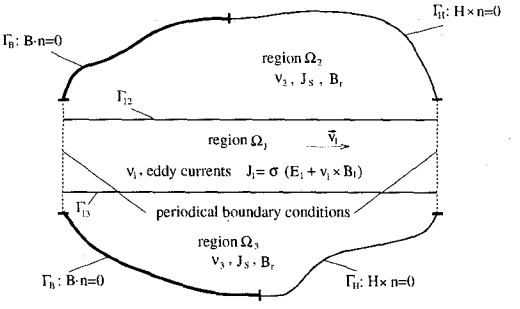

Fig. 3. Magnetostatic field problem with a moving conductor

moving part is invariant in the direction of motion, the Maxwell equations for region Ω_1 are:

$$\left.\begin{aligned} \operatorname{curl}\vec{E} &= \vec{0} && (1)\\ \operatorname{div}\vec{J} &= 0 && (2)\\ \vec{J} &= \sigma\left(\vec{E}+\vec{v}\times\vec{B}\right) && (3)\\ \operatorname{curl}\vec{H} &= \vec{J} && (4)\\ \operatorname{div}\vec{B} &= 0 && (5)\\ \vec{H} &= \nu(B)\,\vec{B} && (6)\end{aligned}\right\} \text{ in } \Omega_1$$

In the non-moving parts of the chosen reference system the excitation of the system may result from either permanent magnets or electrical source currents. All non-moving regions, equal if they represent coils, permanent magnets, non-linear iron or air, obey the Maxwell equations of a magnetostatic field problem and may be combined in Ω_2:

$$\left.\begin{aligned} \operatorname{curl}\vec{H} &= \vec{J}_s && (7)\\ \operatorname{div}\vec{B} &= 0 && (8)\\ \vec{H} &= \nu(B)\,(\vec{B}-\vec{B}_r) && (9)\end{aligned}\right\} \text{ in } \Omega_2$$

The interface boundary conditions between the moving and non-moving part are described as follows:

$$\left.\begin{aligned} \vec{n}\times\left(\vec{H}_1-\vec{H}_2\right) &= \vec{0} && (10)\\ \vec{n}\cdot\left(\vec{B}_1-\vec{B}_2\right) &= 0 && (11)\\ \vec{n}\cdot\vec{J}_1 &= 0 && (12)\end{aligned}\right\} \text{ on } \Gamma_{12}$$

The outer boundary of the model is divided into three parts. In the direction of motion periodical boundary conditions are defined. The other boundary conditions are described by a vanishing normal component of the flux density on Γ_B or a vanishing tangential component of the magnetic field intensity on Γ_H:

$$\vec{n}\cdot\vec{B} = 0 \quad \text{on } \Gamma_B \qquad (13)$$

$$\vec{n}\times\vec{H} = \vec{0} \quad \text{on } \Gamma_H \qquad (14)$$

B. Potential formulations

In order to satisfy equation (1), (5) and (8) the $\vec{A}, V$ formulation is used in Ω_1 and the $\vec{A}$ formulation is used in Ω_2. Choosing these potentials equation (1)-(9) can be written as follows:

$$\begin{aligned} &\operatorname{curl}\nu\operatorname{curl}\vec{A}\\ &\quad-\left(\sigma\vec{v}\times\operatorname{curl}\vec{A}-\sigma\operatorname{grad}V\right) = \vec{0} \quad \text{in } \Omega_1 \qquad (15)\\ &\operatorname{div}\left(\sigma\vec{v}\times\operatorname{curl}\vec{A}-\sigma\operatorname{grad}V\right) = 0 \quad \text{in } \Omega_1 \qquad (16)\\ &\operatorname{curl}\nu\operatorname{curl}\vec{A}-\operatorname{curl}\nu\vec{B}_r = \vec{J}_s \quad \text{in } \Omega_2 \qquad (17)\end{aligned}$$

The boundary conditions (10)-(14) result in:

$$\left.\begin{aligned} \vec{n}\times\left(\nu_1\operatorname{curl}\vec{A}_1-\nu_2\operatorname{curl}\vec{A}_2+\nu_2\vec{B}_{r_2}\right) &= \vec{0} && (18)\\ \vec{n}\cdot\left(\operatorname{curl}\vec{A}_1-\operatorname{curl}\vec{A}_2\right) &= 0 && (19)\\ \vec{n}\cdot\left(\sigma\vec{v}\times\operatorname{curl}\vec{A}_1-\sigma\operatorname{grad}\vec{V}_1\right) &= 0 && (20)\end{aligned}\right\} \text{ on } \Gamma_{12}$$

$$\vec{n}\cdot\operatorname{curl}\vec{A} = 0 \quad \text{on } \Gamma_B \qquad (21)$$

$$\vec{n}\times\left(\nu\operatorname{curl}\vec{A}-\nu\vec{B}_r\right) = \vec{0} \quad \text{on } \Gamma_H \qquad (22)$$

Enforcing the continuity of $\vec{A}$ on Γ_{12} and the tangential component of $\vec{A}$ to be constant on Γ_2 by setting

$$\vec{A}_1 = \vec{A}_2 \quad \text{on } \Gamma_{12} \quad \text{and} \qquad (23)$$

$$\vec{n}\times\vec{A} = \vec{0} \quad \text{on } \Gamma_B\ , \qquad (24)$$

the boundary condition (19) and (21) are automatically satisfied and can be omitted. In fact equation (15)-(18), (20) and (22)-(24) gives a complete potential formulation for equation (1)-(14). But the solution for the potentials is analytically not unique, because the divergence of $\vec{A}$ is still vague.

C. Coulomb gauge

To get a unique solution for the potential $\vec{A}$ the divergence of $\vec{A}$ has to be determined as well as the free normal component of $\vec{A}$ on Γ_2: For this gauge of $\vec{A}$ the Coulomb gauge is chosen in this paper:

$$\operatorname{div}\vec{A} = 0 \quad \text{in } \Omega_1 \text{ and } \Omega_2 \qquad (25)$$

$$\vec{n}\cdot\vec{A} = 0 \quad \text{on } \Gamma_H. \qquad (26)$$

It is important to mention that gauging is not necessary to get a numerical solution for the field problem described by equation (1)-(14), but has an effect on the convergence of the solution process and on the accuracy of the solution.

III. Numerical Implementation

Applying the Galerkin weighted residual method using the shape functions as weighting functions to the second term of (15) leads to:

$$\int_{\Omega_1}\left(\vec{N}_i\cdot\sigma\vec{v}\times\operatorname{curl}\vec{A}\right)d\Omega \qquad (27)$$

This term forces the matrix to be badly posed and causes violent oscillations in the solution process. These oscillations can be enormously reduced by upwinding and additionally by a stabilized BiCG procedure [4]. In regions of high permeability the stability of the solution can be additionally optimized by enforcing the Coulomb gauge. In [5] it is shown that the Coulomb gauge can be obtained in the numerical solution by adding $(\operatorname{grad}\nu\operatorname{div}\vec{A})$ to equation (15) and (17) in region Ω_1 and Ω_2. But the advantage of a better convergence in this case costs accuracy of the field solution especially if the iron regions of the moving parts are not saturated, so that the permeability differences between iron and air are high [6]. The following numerical formulations give 4 possibilities for the solution of the given field problem, which use all the same upwind scheme but differ in the way of implementing the Coulomb gauge. Only for two of them convergence is obtained for the given levitation system in the considered speed range.

A. Formulation without Coulomb gauge

In this case the Coulomb gauge is not implemented, so that the whole FE-formulation looks as follows:

$$\int_{\Omega_1} \Big(\nu \operatorname{curl} \vec{N}_i \cdot \operatorname{curl} \vec{A} - \vec{N}_i \cdot \sigma \vec{v} \times \operatorname{curl} \vec{A} + \vec{N}_i \cdot \sigma \operatorname{grad} V \Big) \, d\Omega = 0 \quad (28)$$

$$\int_{\Omega_1} \Big(\sigma \operatorname{grad} N_i \cdot \vec{v} \times \operatorname{curl} \vec{A} - \sigma \operatorname{grad} N_i \cdot \operatorname{grad} V \Big) \, d\Omega = 0 \quad (29)$$

$$\int_{\Omega_2} \Big(\nu \operatorname{curl} \vec{N}_i \cdot \operatorname{curl} \vec{A} - \nu \operatorname{curl} \vec{N}_i \cdot \vec{B}_r - \vec{N}_i \cdot \vec{J}_s \Big) \, d\Omega = 0 \quad (30)$$

The convergence of the CG procedure for this case is already bad without taking velocity effects into account. Considering small velocities the solution process does not converge.

B. Regular Coulomb gauge

In this case the Coulomb gauge is implemented in Ω_1 and Ω_2 by adding $(\operatorname{grad} \nu \operatorname{div} \vec{A})$ to equation (15) and (17). By additionally enforcing $\vec{n} \cdot \vec{A} = 0$ on Γ_H, $\nu \operatorname{div} \vec{A} = 0$ on Γ_B and the continuity of $(\nu \operatorname{div} \vec{A})$ on Γ_{12} it is shown in [5] that the divergence of $\vec{A}$ in fact vanishes:

$$\nu \operatorname{div} \vec{A} = 0 \quad \text{in } \Omega_1 \text{ and } \Omega_2 \quad (31)$$

In this case the numerical implementation of the entire formulation results in:

$$\int_{\Omega_1} \Big(\nu \operatorname{curl} \vec{N}_i \cdot \operatorname{curl} \vec{A} + \nu \operatorname{div} \vec{N}_i \cdot \operatorname{div} \vec{A} - \vec{N}_i \cdot \sigma \vec{v} \times \operatorname{curl} \vec{A} + \vec{N}_i \cdot \sigma \operatorname{grad} V \Big) \, d\Omega = 0 \quad (32)$$

$$\int_{\Omega_1} \Big(\sigma \operatorname{grad} N_i \cdot \vec{v} \times \operatorname{curl} \vec{A} - \sigma \operatorname{grad} N_i \cdot \operatorname{grad} V \Big) \, d\Omega = 0 \quad (33)$$

$$\int_{\Omega_2} \Big(\nu \operatorname{curl} \vec{N}_i \cdot \operatorname{curl} \vec{A} + \nu \operatorname{div} \vec{N}_i \cdot \operatorname{div} \vec{A} - \nu \operatorname{curl} \vec{N}_i \cdot \vec{B}_r - \vec{N}_i \cdot \vec{J}_s \Big) \, d\Omega = 0 \quad (34)$$

The convergence of the CG procedure without any velocity effects is better than in the formulation of section A, but the accuracy of the results is not as good as in section A. As well as in section A the solution process does not converge considering small velocities because of the high iron permeabilities.

C. Fortified Coulomb gauge

In this case the Coulomb gauge is implemented in Ω_1 and Ω_2 by adding $(\operatorname{grad} \nu_0 \operatorname{div} \vec{A})$ to equation (15) and (17). By additionally enforcing $\vec{n} \cdot \vec{A} = 0$ on Γ_H, $\nu_0 \operatorname{div} \vec{A} = 0$ on Γ_B and the continuity of $(\nu_0 \operatorname{div} \vec{A})$ on Γ_{12} it can be equally shown, that the divergence of $\vec{A}$ vanishes:

$$\nu_0 \operatorname{div} \vec{A} = 0 \quad \text{in } \Omega_1 \text{ and } \Omega_2 \quad (35)$$

Here the entire formulation can be given as follows:

$$\int_{\Omega_1} \Big(\nu \operatorname{curl} \vec{N}_i \cdot \operatorname{curl} \vec{A} + \nu_0 \operatorname{div} \vec{N}_i \cdot \operatorname{div} \vec{A} - \vec{N}_i \cdot \sigma \vec{v} \times \operatorname{curl} \vec{A} + \vec{N}_i \cdot \sigma \operatorname{grad} V \Big) \, d\Omega = 0 \quad (36)$$

$$\int_{\Omega_1} \Big(\sigma \operatorname{grad} N_i \cdot \vec{v} \times \operatorname{curl} \vec{A} - \sigma \operatorname{grad} N_i \cdot \operatorname{grad} V \Big) \, d\Omega = 0 \quad (37)$$

$$\int_{\Omega_2} \Big(\nu \operatorname{curl} \vec{N}_i \cdot \operatorname{curl} \vec{A} + \nu_0 \operatorname{div} \vec{N}_i \cdot \operatorname{div} \vec{A} - \nu \operatorname{curl} \vec{N}_i \cdot \vec{B}_r - \vec{N}_i \cdot \vec{J}_s \Big) \, d\Omega = 0 \quad (38)$$

Because of the high permeability of the iron parts the Coulomb gauge is stronger fortified by adding $(\nu_0 \operatorname{div} \vec{A})$ instead of $(\nu \operatorname{div} \vec{A})$. So the convergence of the CG procedure is considerably better than in the first two formulation. Velocity effects can be considered well. But like in section B the accuracy of the results is not as good as in section A.

D. Fortified Coulomb gauge in moving conductor

In this case the Coulomb gauge is implemented only in the moving part Ω_1 by adding $(\operatorname{grad} \nu_0 \operatorname{div} \vec{A})$ to equation (15). By additionally enforcing $(\nu_0 \operatorname{div} \vec{A} = 0)$ on Γ_{12} it can be similarly shown that the divergence of $\vec{A}$ vanishes in Ω_1:

$$\nu_0 \operatorname{div} \vec{A} = 0 \quad \text{in } \Omega_1 \quad (39)$$

So the entire formulation can be described by:

$$\int_{\Omega_1} \Big(\nu \operatorname{curl} \vec{N}_i \cdot \operatorname{curl} \vec{A} + \nu_0 \operatorname{div} \vec{N}_i \cdot \operatorname{div} \vec{A} - \vec{N}_i \cdot \sigma \vec{v} \times \operatorname{curl} \vec{A} + \vec{N}_i \cdot \sigma \operatorname{grad} V \Big) \, d\Omega = 0 \quad (40)$$

$$\int_{\Omega_1} \Big(\sigma \operatorname{grad} N_i \cdot \vec{v} \times \operatorname{curl} \vec{A} - \sigma \operatorname{grad} N_i \cdot \operatorname{grad} V \Big) \, d\Omega = 0 \quad (41)$$

$$\int_{\Omega_2} \Big(\nu \operatorname{curl} \vec{N}_i \cdot \operatorname{curl} \vec{A} - \nu \operatorname{curl} \vec{N}_i \cdot \vec{B}_r - \vec{N}_i \cdot \vec{J}_s \Big) \, d\Omega = 0 \quad (42)$$

The convergence of the solution process is better than in the first two formulations so that velocity effects can be considered. Because of the more accurate formulation in the non-moving parts the accuracy of the results are better than in section C.

IV. Results

The considered mesh of the hybrid levitation magnet shown in Fig. 2 consists of about 50000 first order tetrahedral elements with 10000 nodes and about 32000 degree of freedoms using the $\vec{A}$, V- $\vec{A}$ formulation. Calculations

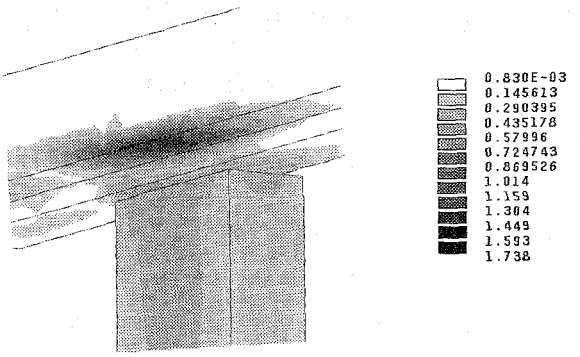

Fig. 4. Absolute value of $\vec{B}$ at 5 m/s ($\theta = 0$ A)

were done for the 4 formulations once with a permanent magnet excitation and once with a hybrid excitation with a total number of ampere turns $\theta = -600$A. Fig. 4,5 and 6 show the numerical field solutions of the flux density value, the resulting eddy currents and the electrical scalar potential V in the rail. It is recognizable, how the flux density refuses to follow the excited field and how the distribution of the eddy currents has to look like to cause this effect of resistance against changes of the exciting field. Fig. 7 and 8 display the attractive and braking force curves calculated by the Maxwell stress tensor for the 4 different gauging methods in the $\vec{A}$, V- $\vec{A}$ formulation compared with a scalar potential formulation, which leads to the best result in the non-moving case compared to measurements. As pointed out in section 3 only the two $\vec{A}$, V- $\vec{A}$ formulations with the fortified Coulomb gauge converge over the full speed range. Formulation III C needs twice as much CG-steps for each non-linear calculation step as formulation III D, but this formulation impresses with its accuracy compared to formulation III A without upwinding and Coulomb gauge.

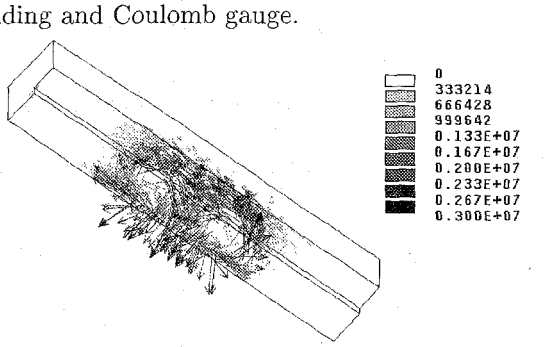

Fig. 5. Induced currents $\vec{J}$ in the rail at 5 m/s ($\theta = 0$ A)

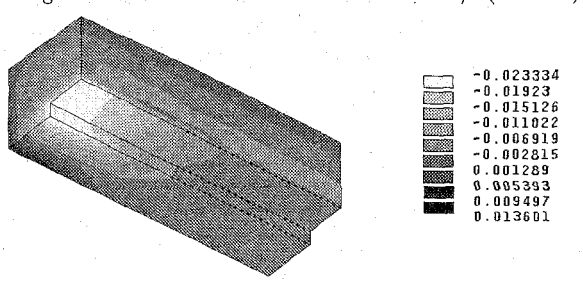

Fig. 6. Electric Scalar Potential V in the rail at 5 m/s ($\theta = 0$ A)

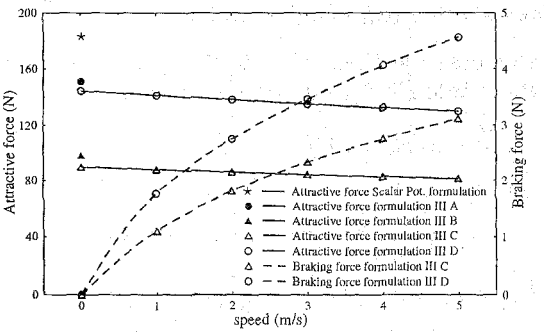

Fig. 7. Attractive and braking forces for $\theta = 0$ A

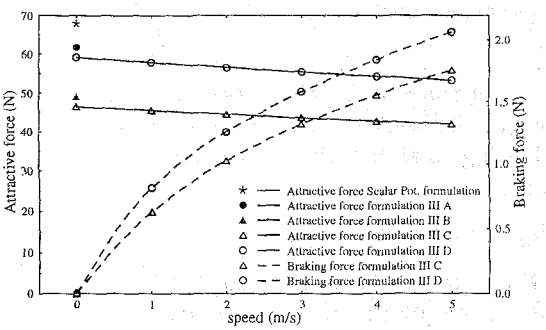

Fig. 8. Attractive and braking forces for $\theta = -600$ A

V. Conclusions

In this paper a complete formulation is given to solve magnetic moving conductors eddy current field problem excited by either permanent magnets or electrical source currents. Dependencies of the convergence and the accuracy on the implementation of the Coulomb gauge are described. The given formulation with four different gauging methods was applied to a magnetic levitation system to compute its electromagnetic field, induced currents and forces and to compare the different calculation methods.

References

[1] C. Reuber, D. Rödder, G. Henneberger, "Position Control of a Magnetically Suspended Carrier with a Permanent-Excited Linear Synchronous Machine", *14th International Conference on Magnetically Levitated Systems, MAGLEV95*, Bremen, November 1995.

[2] D. Albertz, S. Dappen, G. Henneberger, "Calculation of the 3D Non-linear Eddy Current Field in Moving Conductors and its Application to Braking Systems", *IEEE Trans. Magn.*, vol. 32, no.3, pp. 3145-3159, 1989.

[3] D. Albertz, S. Dappen, G. Henneberger, "Combination of 2D and 3D Non-Linear Eddy Current Calculations for the Design of Braking Systems", *Proceedings of The International Symposium on Non-Linear Electromagnetic Systems (ISEM, Cardiff 1995)*, IOS Press, Amsterdam.

[4] H. A. van der Vorst, "BI-CGSTAB: A fast and smoothly converging variant of BI-CG for the solution of nonsymmetric linear systems", *SIAM J. Sci. Stat. Comput.*, vol. 13, no 2, pp. 631-644, 1992.

[5] O. Biro, K. Preis, "On the Use of Magnetic Vector Potential in the Finite Element Analysis of Three-Dimensional Eddy Currents", *IEEE Trans. Magn.*, vol. 25, no 4, pp. 3145-3159, 1989.

[6] K. Preis, I. Bardi, O. Biro, C. Magele, W. Renhart, K. R. Richter, G. Vrisk, "Numerical analysis of 3D magnetostatic fields", *IEEE Trans. Magn.*, vol. 27, no 5, pp. 3798-3803, 1991.